

Observations of a negatively buoyant river plume in a large lake

James H. Churchill

Department of Physical Oceanography, Woods Hole Oceanographic Institution, Woods Hole, Massachusetts 02543

Elise A. Ralph and Angela M. Cates

Large Lakes Observatory, University of Minnesota at Duluth, Duluth, Minnesota 55812

Judith W. Budd

Department of Geological Engineering and Sciences, Michigan Technological University, Houghton, Michigan 49931

Noel R. Urban

Department of Civil and Environmental Engineering, Michigan Technological University, Houghton, Michigan 49931

Abstract

Although seldom studied, negatively buoyant river plumes may be common within large lakes, especially during spring when lake and river waters are near the temperature of maximum fresh water density (4°C) and relatively warm river discharge can be denser than the receiving lake water. Here we examine a negatively buoyant plume entering Lake Superior from the Ontonagon River during late March 2000. Because of small temperature related density differences, the sediment load carried by the river made an appreciable contribution to the plume-edge density field and significantly impacted plume-edge dynamics. Particle-related density gradients were responsible for roughly one-third of the geostrophic velocity shear at the plume edge. As a result of the small width (50 m) of the Ontonagon River mouth, the emerging river water was not deflected by rotational effects. Its movement appeared to have been primarily controlled by the wind-driven coastal current. Our analysis indicates that the frequent reversals of this current should effectively limit the plume's alongshore extent and may result in a continuous coastal band of turbid water extending alongshore in either direction from the river mouth.

The behavior of an estuarine discharge plume, as well as the fate of material it carries, is strongly influenced by its density relative to receiving waters. By far, the majority of scientifically scrutinized river discharge plumes have been positively buoyant relative to the surrounding waters (e.g., Bowman and Iverson 1977; Boicourt et al. 1987; Garvine 1995; Hickey et al. 1998). However, a negatively buoyant river discharge plume may not be a rarity. In the coastal ocean, the density of exiting estuarine water may exceed that of receiving ocean water due to a heavy sediment load (as seen off the Huanghe river; Wright et al. 1986) or due to high salinities produced by excessive evaporation within an embayment (as seen off Spencer Gulf Australia; Nunes Vaz

et al. 1990). In large lakes, where water density is controlled principally by temperature and sediment concentration, negatively buoyant discharge plumes may be relatively common. For example, falling air temperatures may produce a river discharge that is colder and denser than the receiving lake water. Masse and Murthy (1990) observed a discharge plume of this type entering Lake Ontario from the Niagara River. During late winter and early spring, when large lake temperatures are often less than 4°C (temperature of maximum density in fresh water), relatively warm river water may form a negatively buoyant plume within colder lake water. This sort of plume could be common during times of maximum volume and sediment discharge from a river and, thus, may be particularly important when considering the transport of river-borne solids.

Acknowledgments

We must extend special thanks to Captain M. King and the crew of the R/V *Blue Heron* (R. Lauby, R. Scott, and J. Simenson) for their efforts during the survey work. We are also grateful to C. Wittkop and M. Zapp King for assistance in CTD and drogue tracking operations. We are indebted to M. Auer of Michigan Technical University for his assistance and advice during the course of our study. For their helpful recommendations on improving this manuscript, our gratitude is extended to J. O'Donnell of the University of Connecticut, G. Gawarkiewicz of the Woods Hole Oceanographic Institution, Derek Fong of Stanford University, and an anonymous reviewer. The work described was part of the Keweenaw Interdisciplinary Transport Experiment in Superior funded by the National Science Foundation through grants 9712889 to J.C., 9712871 to E.R., 9712872 to J.B., and 9712872 to N.U. Woods Hole Oceanographic Institution contribution number 10492.

Here we present what may be the first observations of a warm, negatively buoyant river plume entering a Laurentian Great Lake. They were acquired in late March 2000 within an area of Lake Superior near the Ontonagon River mouth (Fig. 1). The data set consists of vertical profiles of temperature and optical transmission, suspended particulate concentrations (from water samples), surface drifter tracks, and water velocity time series. Using these measurements, we examine near- and far-field properties of the river plume and an associated coastal band of turbid water. Also examined are the dynamics in plume's frontal region and the manner in which the emerging plume is influenced by the Earth's rotation and the wind-driven coastal current. We first describe the study region and measurement procedures.

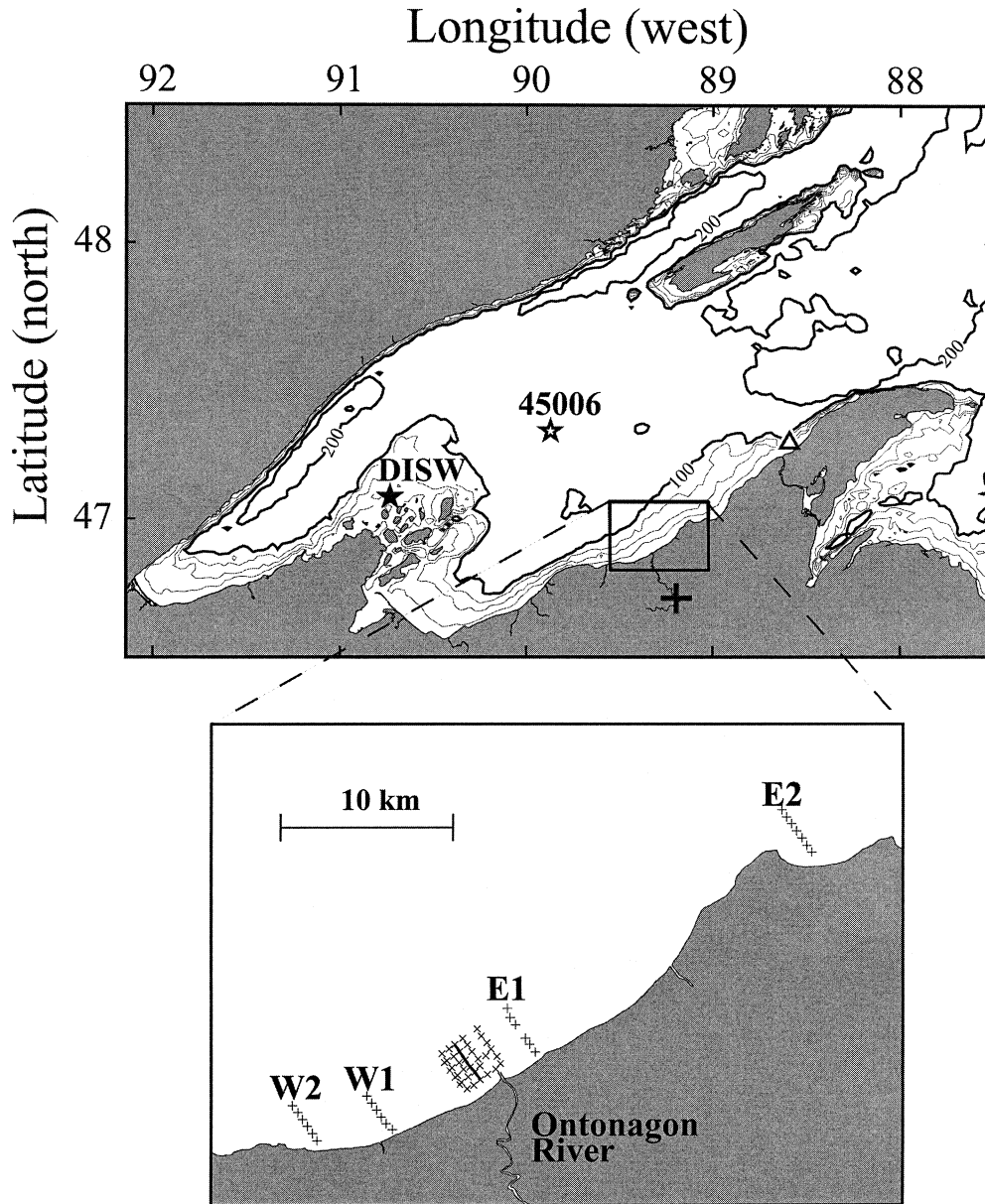


Fig. 1. Western Lake Superior and the study region near the Ontonagon River mouth. Crosses show the location of selected CTD stations occupied over 30–31 March 2000. The location of a current meter, whose data were used in our analysis, is marked by a triangle. Also shown are meteorological stations (stars) and the location of a stream flow gauge (maintained by the U.S. Geological Survey) on the Ontonagon (cross). In the larger scale plot, the depth contours are at 25, 50, 75, 100, and 200 m.

Measurements

Site description—The Ontonagon River empties into Lake Superior near the base of the Keweenaw Peninsula (Fig. 1), a spit of land that extends into the southern lake. Entry of the river water into the lake is through the end of a navigation channel. Lined by breakwaters, the channel has a width of 50 m and a mean depth of 6.4 m and extends 360 m from the lakeshore. The lake floor off the Ontonagon River mouth and the rest of the lower Keweenaw Peninsula slopes relatively gently offshore, with an incline of roughly

0.007. Off the middle peninsula, bottom slopes are more variable and the lake floor may be divided into two regions: a gently sloping shelf, with a bottom incline of roughly 0.008, extending to about the 30-m isobath, and a slope with an incline of roughly 0.035 further offshore.

In a recent study, Gatzke (2001) examined the properties of rivers emptying into Lake Superior over a region, from Odanah, Wisconsin, to Copper Harbor, Michigan, which includes the eastern Keweenaw. He found the Ontonagon River to be the largest hydrologic source of this region, contributing 32% of the annual tributary flow (1989–1998).

According to his analysis, the Ontonagon ranks second as a source of suspended solids from runoff to the region, contributing 29% of the annual runoff load.

Previous investigators have noted the presence of a strong northeastward coastal current off the Keweenaw Peninsula, commonly referred to as the Keweenaw current (Ragotzkie 1966; Viekman and Winbush 1993). A numerical modeling investigation by Chen et al. (2001) and Zhu et al. (2001) has indicated that this is, in part, a thermally driven current caused by rapid warming of nearshore (vs. offshore) water.

Our examination of the Ontonagon discharge is part of the Keweenaw interdisciplinary transport experiment in Superior (KITES). A preliminary analysis of the moored current meter data from KITES indicates that the Keweenaw current is a seasonal feature, appearing principally in the summer and autumn. This analysis further indicates that during spring, the time of the Ontonagon discharge study described here, flow off the Keweenaw Peninsula is principally driven by the surface wind stress and has a mean of close to zero. A brief examination of a portion of the KITES current meter data set, focusing on the effects of coastal flow on the discharge plume, is given in the Analysis section.

CTD survey—The temperature profiles used in our study came from a conductivity–temperature–depth (CTD) survey conducted near the Ontonagon River mouth (Fig. 1) during 30–31 March 2000. Surveying was done from the R/V *Blue Heron*, operated by the University of Minnesota at Duluth. The CTD (Seabird SBE-9) was attached to a nine-bottle rosette sampler and equipped with a 25-cm transmissometer (Wetlabs, C-Star). The 159 CTD stations of the survey may be divided into two subsurveys. During 30 March, we carried out a near-field survey of the river plume, occupying seven transects within 2.5 km of the river mouth. This was followed by a larger scale survey of the region, which included transects more than 20 km from the river mouth.

To convert the transmissometer signal to suspended particle concentration, P , we obtained a total of 14 water samples from various locations and depths using the rosette sampler. For each sample, a volume of 1.7 to 8.5 liters was filtered through a 0.7- μm mesh filter to give total P . The results showed a near linear relationship between P and coincident measurements of percent transmission. Linear regression of these two variables yielded a correlation (R^2) of 0.98 and the following relationship:

$$P = -0.0985T + 7.78$$

where P is in mg L^{-1} and T is percent transmission. Because the transmissometer signal was saturated (at a constant 0% transmission) at particle concentrations in excess of 7.78 mg L^{-1} , this relationship is valid only for $0 < P < 7.78 \text{ mg L}^{-1}$. As discussed further below, the inability to resolve variations of $P > 7.78 \text{ mg L}^{-1}$ did not seriously limit our view of particle concentrations, or particle-related dynamics, at the edge of the Ontonagon River plume.

During the near-field CTD survey, we deployed surface drifters in the plume-edge region. These were rigged as Davis-style drifters (Davis 1985), designed to follow the flow over the surface 1 m. Drag was supplied by four 0.5- by 0.9-m sails radiating from the drifter's central electronics

case. Each drifter was equipped with a GPS receiver. Also attached to each drifter was an ARGOS PTT, which enabled communication of positions to system ARGOS and to a tracking system onboard the R/V *Blue Heron*.

Following Churchill et al. (1999), drifter velocities were computed through linear regression of drifter position with time. The regression of a position component against time was carried out in a data window containing a specified number of drifter fixes. Slope of the regression line was taken as the estimate of velocity component at the middle of the window. Stepping the regression window through the position component time series gave a velocity component time series. The velocities computed by this method had 90% confidence intervals (of the regression slope) of roughly 1 cm s^{-1} .

Time series measurements—As part of our analysis of wind-driven alongshore flows, we examined water velocities measured by a current meter set 4.5 m above bottom on a tripod 60 km northeast of the Ontonagon River mouth (Fig. 1). This was part of an array of acoustic travel time current meters (Williams et al. 1987) set out to study near-bottom sediment and fluid dynamics over the Keweenaw shelf and upper slope.

Winds used in our analysis came from NOAA buoy 45006 and the Devils Island C-MAN station (labeled 45006 and DISW, respectively, in Fig. 1). The wind velocities from these two stations were highly correlated. For example, 1999 alongshore wind speeds (along the orientation of the middle Keweenaw) from these stations were correlated at $R^2 = 0.89$. Only the C-MAN station was operational during the CTD survey. Winds from buoy 45006 were used in the analysis of the acoustic travel time current meter data cited above. For both station time series, wind speed was converted to surface wind stress using the formulae of Wu (1969).

Estimates of the Ontonagon River transport to be presented were from a stream flow gauge maintained by the U.S. Geological Survey (USGS) near Rockland, Michigan (Fig. 1).

Results

River discharge and wind conditions—The CTD survey had been scheduled for late March because this is, historically, the time of peak Ontonagon discharge. However, the USGS stream flow data show that the mild winter of 1999–2000 resulted in a comparatively weak and early maximum discharge. In the 2000 stream flow record from Rockland, Michigan, the peak transport of roughly $200 \text{ m}^3 \text{ s}^{-1}$ occurs in late February (Fig. 2). A secondary discharge maximum of roughly $150 \text{ m}^3 \text{ s}^{-1}$ precedes our CTD survey by roughly 3 d. In contrast, in the Rockland stream flow record of 1997, a year with a comparatively wet and cold winter, the maximum transport of $450 \text{ m}^3 \text{ s}^{-1}$ occurs in early April.

The Devils Island C-MAN record (Fig. 3) shows strong and variable winds over the week prior to our survey. Southwest winds (directed to the northeast) $>15 \text{ m s}^{-1}$ appear in the record on 25 March (not shown in Fig. 3), while north winds of $>12 \text{ m s}^{-1}$ are seen on 28 March. Much less severe conditions are seen during the time of the CTD survey. Very

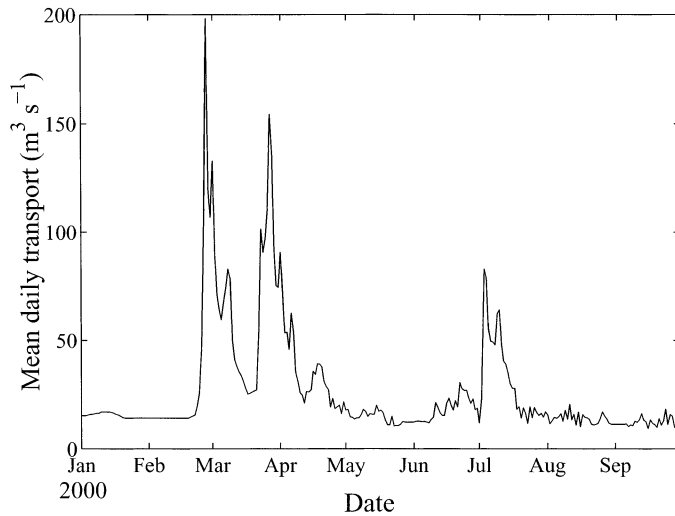


Fig. 2. Mean daily Ontonagon River flow for 2000 measured at the Rockland, Michigan, stream flow gauge (Fig. 1).

weak winds, of $<3 \text{ m s}^{-1}$, persist throughout the period of near-field survey on 30 March.

Near-field plume conditions—Horizontal fields of temperature and P , derived from the near-field CTD survey data, show a band of warm and turbid water confined to the coastal region near the river mouth (Fig. 4). In the P fields, there is an especially clear demarcation between this band and the relatively clear lake water offshore. The distributions of P also show the band to be a narrow feature, extending no more than 3 km from the coast over the entire survey region.

Vertical fields of temperature and P over the survey's central transect (Fig. 5) reveal that the band is bound offshore by a surface to bottom turbidity and temperature front. Unlike the front typically seen at the edge of a positively buoy-

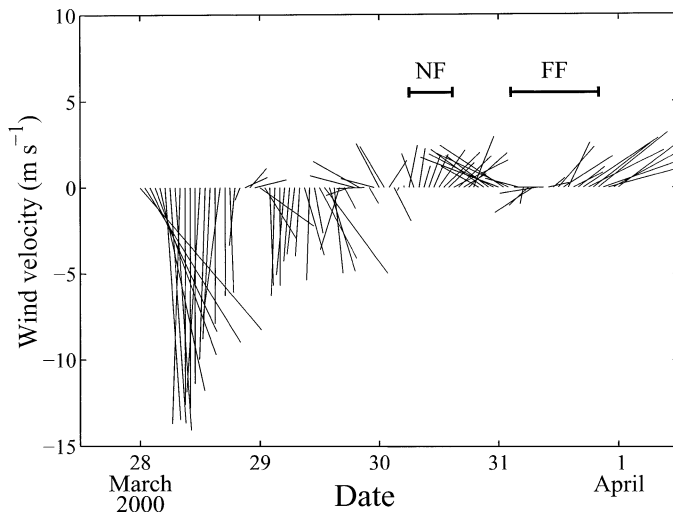


Fig. 3. Wind velocities of late March 2000 measured at the Devils Island C-MAN station (Fig. 1). The measurement level is 25 m above lake level. The horizontal lines mark the periods of the near-field (NF) and far-field (FF) surveys. The coordinate system is geographic with northward winds directed vertically upward.

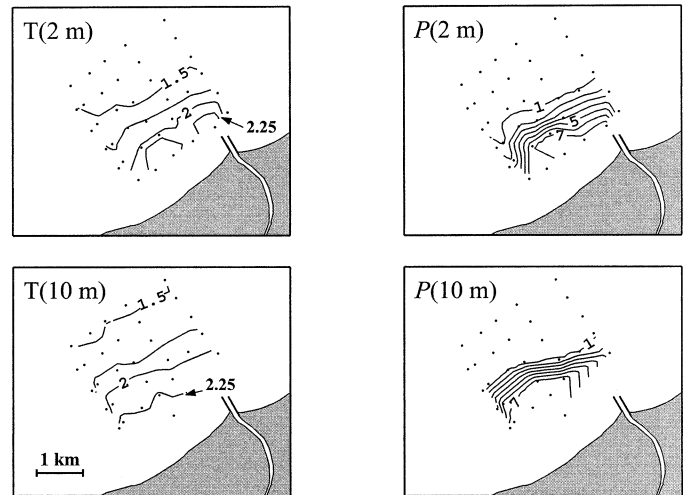


Fig. 4. Distributions of temperature, T ($^{\circ}\text{C}$), and suspended particle concentration, P (mg L^{-1}), at 2 and 10 m derived from measurement of the 30 March 2000 CTD survey. CTD station locations are shown as dots.

ant discharge plume, which tends to slope upward going offshore (e.g., Munchow and Garvine 1993), the front seen in this section slopes sharply downward going offshore. As revealed by the depths of the $P = 1$ and $P = 4 \text{ mg L}^{-1}$ surfaces (Fig. 6), the plume descends rapidly to the bottom over the entire survey region. Even where its slope is the smallest, at the survey's southwestern edge, the plume extends from the surface to the bottom over an across-shore distance of less than 1.5 km.

A southwestward surface current in this frontal region is revealed by the tracks of the two drifters set out on either side of the front early in the near-field survey (Fig. 7). After their release near the eastern edge of the survey region, both drifters move alongshore to the southwest at a speed of

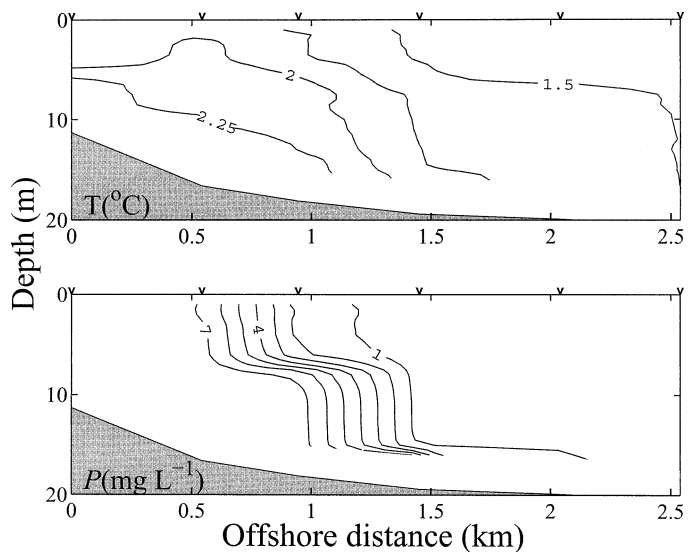


Fig. 5. Vertical distributions of temperature and P along the central transect of the near-field survey (marked by a solid line in Fig. 1). Station locations are indicated by "v" on the upper axis.

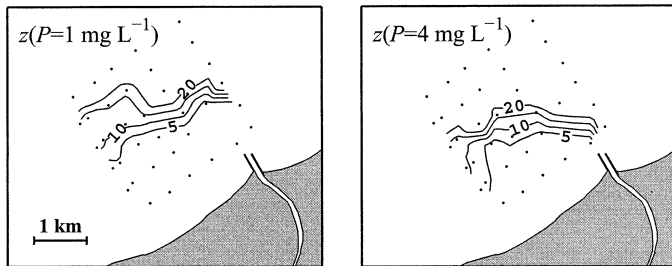


Fig. 6. Same as Fig. 4, except showing depths, z , of the $P = 1$ and $P = 4 \text{ mg L}^{-1}$ surfaces.

roughly 6 cm s^{-1} . It is notable that the drifter tracks are nearly parallel. Convergence has been observed at the edge of buoyant river plumes in the marine environment (Garvine and Monk 1974; O'Donnell et al. 1998). Our drifter tracks, however, show no evidence of convergence, or divergence, in the frontal region of the turbid water band off the Ontonagon River mouth.

The drifter tracks roughly follow the contours of the near-surface front as outlined by the 2-m P field (Fig. 4). A careful examination of this field suggests that the turbid water band appearing in the near-field survey has two sources: highly turbid water issuing from the Ontonagon and moderately turbid fluid entering the survey region from the northeast. Contours of $P > 4 \text{ mg L}^{-1}$ give evidence of the first source. These appear to extend from the river mouth and veer sharply to the southwest. By contrast, the $1\text{--}3 \text{ mg L}^{-1}$ contours show no veering toward the river mouth but extend across the survey region at an orientation roughly parallel to the shore. This suggests that the origin of near-surface water with P in the $1\text{--}3 \text{ mg L}^{-1}$ range is from the northeast (the upstream direction according to the drifter tracks and the veering of the $P > 4 \text{ mg L}^{-1}$ contours).

What may be a clearer indication of a dual source to the turbid band of the near-field survey is provided by the depths of the $P = 1$ and $P = 4 \text{ mg L}^{-1}$ surfaces (Fig. 6). Depth contours of the 4 mg L^{-1} surface clearly converge toward the river mouth, whereas the 1 mg L^{-1} depth contours show no deflection toward the river mouth but extend in the along-shore direction across the survey region.

Far-field plume conditions—Data of the far-field CTD survey reveal near-shore filaments of warm and turbid water both to the southwest and to the northeast of the Ontonagon River mouth. The pattern of turbidity is consistent with the notion that the turbid water band seen southwest of the river mouth is a combination of river discharge and moderately turbid water from the northeast of the river mouth. The principal aspect of this pattern is that particle concentrations seen southwest of the river mouth are much higher than particle concentrations seen at similar distances northeast of the river mouth (Fig. 8). For example, particle concentrations observed at a transect 2.5 km northeast of the river mouth peak at 5 mg L^{-1} , whereas particle concentrations in excess of 7.8 mg L^{-1} (the maximum concentration observable with the transmissometer) appear at transects 8 and 12 km to the southwest of the river mouth.

The possible origins of the warm and turbid water band

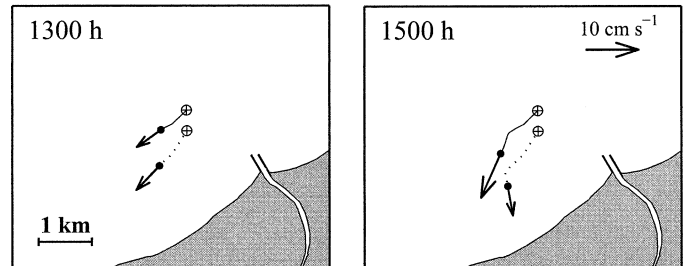


Fig. 7. Positions and velocities of surface drifters at the designated times (GMT on 30 March 2000). Drifters were released during the near-field survey at the positions denoted by the cross-hair symbols. Their tracks are shown as dashed and solid lines.

seen to the northeast of the Ontonagon River mouth, presumably in the upstream direction, are worthy of consideration. The band could be the result of shoreline erosion combined with preferential heating of near-shore waters. Alternatively, it could be Ontonagon discharge water advected to the northeast prior to the most recent near-shore

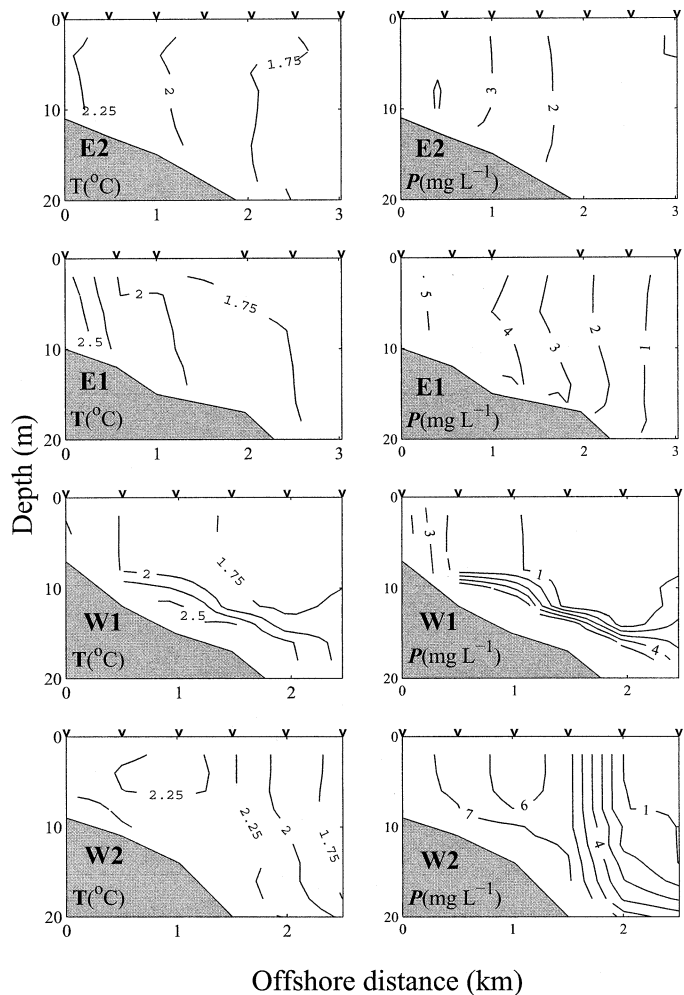


Fig. 8. Distributions of temperature and P along four transects of the 31 March 2000 far-field CTD survey. Transect locations are shown in Fig. 1.

Table 1. Magnitudes of terms of the across-front momentum balance. The magnitudes of all terms are relative to term c , the Coriolis acceleration of the along-front velocity.

Term	Expression	Magnitude
b	$v\partial_y v$	0.031
e	$\tau_y^s/(\rho_0 H)$	0.036
f	$\tau_y^b/(\rho_0 H)$	0.004

current reversal. Consistent with this second possibility is a monotonic decline in the band's maximum P with increasing distance from the Ontonagon River mouth (Fig. 8).

Analysis

Frontal region dynamics—Our data provide a reasonably detailed view of conditions at the edge of the turbid water band appearing in the near-field survey. Data from this region include a sampling of surface velocities derived from the drifter tracks, temperature profiles, and P profiles derived from transmissometer data within the working range of the instrument. These measurements enable us to examine the momentum balance at the edge of the band and estimate the extent to which the suspended particle load contributes to across-shore pressure gradients in this region.

In depth integrated form, the quasi-steady across-stream momentum balance (with acceleration of the across-front velocity assumed to be negligible) at a front may be written as

$$\begin{array}{cccccc}
 u\partial_x v + v\partial_y v + fu + \frac{\partial_y p}{\rho_0} = \frac{\tau_y^s}{\rho_0 H} - \frac{\tau_y^b}{\rho_0 H} \\
 a \quad b \quad c \quad d \quad e \quad f
 \end{array}$$

where x is the along-front coordinate, u is the along-front velocity, v is the across-front velocity, p is pressure, f is the Coriolis parameter, H is the water depth, ρ_0 is a reference density, τ_y^s is the surface wind stress component across the front, and τ_y^b is the across-front bottom stress component.

Using the near-field survey data and the Devils Island wind record, we have estimated the magnitude of terms b , c , e , and f above. The calculation focused on the middle of the survey region and on the time when the drifters traversed this area (1200–1300 h on 30 March). Cross-shelf drifter velocities were essentially constant over this period, varying by much less than the velocity uncertainty of 1 cm s^{-1} . The along-front orientation, x , was determined from the 2-m P field (Fig. 4). It was assumed that the depth-averaged velocities and velocity gradients were half of their values at the surface. The bottom stress was computed according to $\tau_y^b = \rho_0 C_d v |v|$, where $C_d = 0.0025$ (Luketina and Imberger 1987; Masse and Murthy 1990). H and ρ_0 were set to 20 m and $1,000 \text{ kg m}^{-3}$, respectively.

The results (Table 1) indicate that the Coriolis acceleration term, c , is at least 25 times greater than terms b , e , and f . Thus, c can only be balanced by terms a and/or d . Although our data do not permit computation of a , we may assign it an upper limit based on the drifter data and the assumption that the across-front velocity gradients should be considerably larger than the along-front velocity gradients (O'Donnell et al. 1998; Gawarkiewicz et al. 2001). Setting

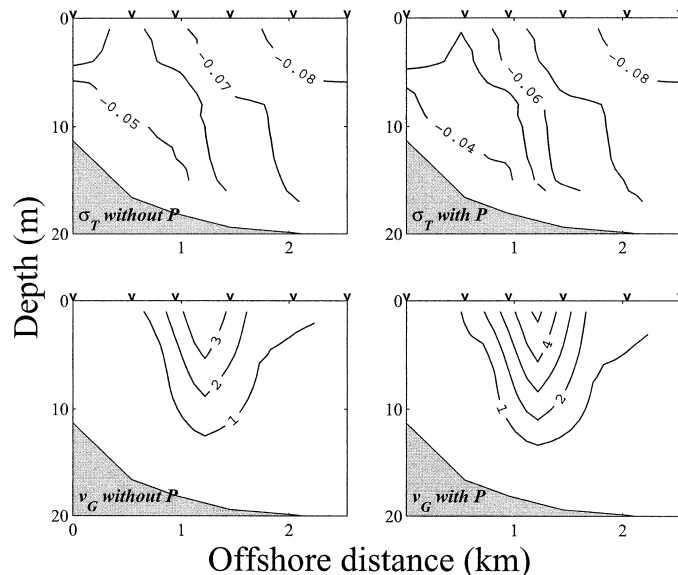


Fig. 9. Vertical profiles of σ_T and computed geostrophic velocity (v_G) along the central transect of the near-field survey (marked by a solid line in Fig. 1). Panels to the left show σ_T and v_G computed without including the contribution of suspended particles, and panels to the right show these properties computed with the contribution of suspended particles.

$\partial_x v$ to 0.3 times the estimate of $\partial_y v$, a reasonable upper limit for $\partial_x v$, and determining u from the drifter velocities gives a magnitude for a that is less than the estimate of c by a factor of 35. Together with the results in Table 1, this indicates that the across-front momentum balance in the target region and time period is nearly geostrophic, e.g., a close balance between the Coriolis acceleration, c , and the across-front pressure gradient, d . This balance is undoubtedly a partial upshot of the weak winds occurring near-field survey (Fig. 3). Over the time period of our analysis, the estimated mean across-front wind stress component is a mere $2.5 \times 10^{-3} \text{ N m}^{-2}$. During periods of stronger wind, we may expect term e to contribute significantly to the momentum balance.

The pressure gradient in the momentum balance is the sum of contributions from the across-front lake surface slope and across-front pressure gradients due to density variations across the front. For this reason, it is of interest to investigate the contribution of the suspended particle load to the across-front density gradient. If this contribution is significant, changes in sediment load, due to particle settling or resuspension, may significantly alter the dynamic balance in the frontal region, especially during periods of weak winds when this balance may be close to geostrophic.

To assess the impact of suspended particles on the across-front density gradient, we have computed density as a function of temperature alone (Chen and Millero 1986) and with the contribution of suspended particles. The results (Fig. 9) indicate that suspended particles increase the across-front density gradient by a factor of roughly 50%.

To further investigate the effect of particles on frontal region dynamics, we have used the survey data to compute geostrophic velocity fields with and without suspended particles contributing to density. The computation was done in

the typical fashion, using densities from adjoining stations on a transect to compute a velocity profile between the stations. It should be noted that because no reference level of zero geostrophic motion could be specified, the computed velocity profiles represent relative (and not absolute) geostrophic currents (i.e., velocity difference between vertical levels). The geostrophic velocities shown here are relative to the current at the deepest common level of the density profiles used in the computation of the velocities (15–17 m at all but the two most inshore station pairs).

Both fields of geostrophic velocity (computed with and without the contribution of suspended particles) show a maximum of alongshore current in the frontal region (Fig. 9). Relative to the deep flow, this current is directed to the southwest. Density gradients due to suspended particles are responsible for a sizeable portion of this flow. For example, the maximum geostrophic current computed using the central transect's data increases from 4 to 5.5 cm s⁻¹ with the inclusion of suspended particles in the calculation (Fig. 9). We note that the computed velocities in the frontal region, where the above-cited maximum occurs, are not sensitive to the limits of the transmissometer's range, due to its saturation at 7.8 mg L⁻¹. All of the transmissometer profiles from the frontal region are within the instrument's range of operation. Further shoreward, however, the transmissometer measurements are often at the saturation level, so that the computed density gradients and geostrophic velocities in this region are unrealistically low.

To obtain a survey-wide view of the effect of density variations on the flow field, we have computed a field of dynamic height at the surface relative to 10 dbar. This gives a sense of the pattern of geostrophic currents at the surface. If 10 m were the true level of zero current and the momentum balance were truly geostrophic, flow at the surface would follow the dynamic height contours and its magnitude would be proportional to the spacing of the contours. The computed dynamic height field (Fig. 10) shows a band of maximum offshore gradients in the region of the plume edge. The contours in this band are orientated roughly alongshore over the central portion of the survey and veer onshore at the western end of the survey. As indicated by Fig. 9, geostrophic velocities following these contours would be directed to the southwest (to the right of the declining gradient in dynamic height). The dynamic height contours also offer further evidence of two sources of inflow to the survey region, discharge from the Ontonagon and alongshore flow from the northeast.

It is noteworthy that the drifter tracks very nearly follow the contours of dynamic height in the band of maximum dynamic height gradient (Figs. 7 and 10). In a manner similar to the dynamic height contours, the drifter tracks veer onshore at the western end of the survey region. In addition, the drifter velocities in the middle of the survey region are about 6 cm s⁻¹, nearly matching the near-surface geostrophic velocities computed from the central transect's data (Fig. 9). These observations may be taken as further evidence of a near-geostrophic momentum balance at the edge of the turbid water band during the near-field survey.

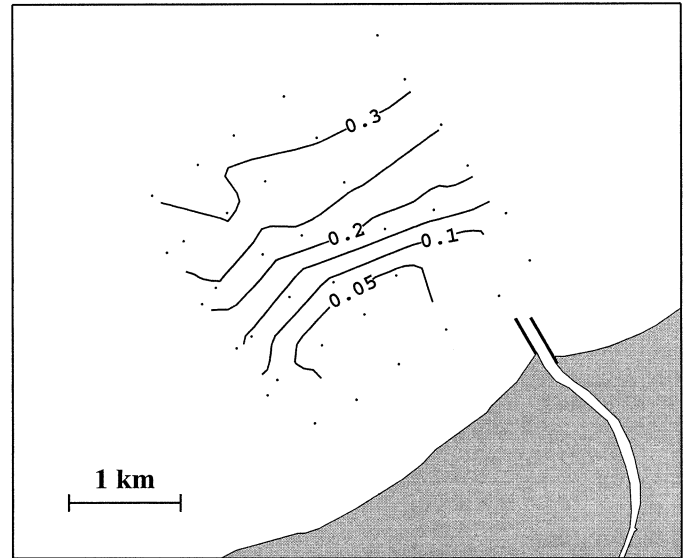


Fig. 10. Same as Fig. 4, except showing dynamic height at the surface relative to 10 m.

The influence of Earth rotation on near-source plume dynamics—Discharge plumes are often classified as rotational or nonrotational, depending on the extent to which dynamics of the emerging plume are influenced by the Earth's rotation. When entering still water, a rotational discharge plume is deflected (anticyclonically in the northern hemisphere) due to the acceleration of its flow generated by the Earth's rotation. By contrast, a nonrotational plume experiences little or no deflection upon entering still water. The extent to which near-source plume dynamics are influenced by Earth's rotation may be roughly quantified by the Kelvin number (Garvine 1987, 1995; Masse and Murthy 1990). For a discharge exiting a river mouth of width, w , this is defined as

$$K = w/r$$

where r is the internal Rossby radius of deformation. Small values of K ($\ll 1$) are indicative of a nonrotational plume, whereas values of K near 1 or larger indicate a significant impact of rotation on plume dynamics.

In the stratified region of the plume, with upper and lower layers of different density, r may be defined as (Csanady 1982)

$$r = [\Delta\rho g h_1 h_2 / (\rho_a (h_1 + h_2))]^{1/2} / f$$

where g is the gravitational acceleration, ρ_a is the mean water density, $\Delta\rho$ is the density difference between the upper and lower layers, and h_1 and h_2 are the layer depths. Using $\Delta\rho$, h_1 , and h_2 determined from density profiles near the river mouth (and at stations where the transmissometer signal is not saturated), we calculate r values on the order of 500 m. With $w = 50$ m, this gives K of order 0.1, leading to the conclusion that the Ontonagon discharge, as it emerges from the river mouth, may be classified as nonrotational.

To further assess the influence of Earth's rotation on the initial deflection of the Ontonagon discharge, it is useful to consider how a negatively buoyant rotational plume behaves

in numerical model simulations. In a recent modeling study, Chao (1998) examined the motion of negatively buoyant, sediment laden, river water emptying into a coastal region with initially motionless fluid of constant density. In the model, a two-layer circulation is formed. The lower layer contains the river discharge water, which turns anticyclonically upon emerging from the river mouth. Farther down the coast the discharge water forms a coastal current with the shore on its right looking down current. The upper layer contains the receiving oceanic water moving within a cyclonic gyre.

Our observations of the Ontonagon discharge plume dramatically differ from the modeled plume behavior. Most significant is that the near-field CTD data and drogue tracks show the discharge water turning cyclonically upon emergence from the river mouth.

Effects of wind forcing—In view of the above findings, the deflection of the Ontonagon discharge plume, seen in the near-field survey, may not be attributed to rotational veering of the plume, but is most likely due to the action of a south-westward coastal current entering the near-field survey region from the northeast. As noted above, analysis of current meter data show that coastal currents off the Keweenaw Peninsula are principally wind driven during early spring. The southwestward current seen during our near-field survey, and presumably responsible for the observed plume deflection, is most likely the product of strong southward winds ($5\text{--}14\text{ m s}^{-1}$) apparent in the Devils Island wind record over the 2 d prior to the near-field survey (Fig. 3).

It is reasonable to conclude that the wind-driven coastal current over the Keweenaw shelf may be a principal agent controlling the movement of the Ontonagon discharge plume during spring. To study the effects of winds on near-shore currents over the Keweenaw shelf, we have employed the records of the acoustic travel time current meter cited in the Measurements section. Although the Ontonagon River mouth and the current meter site are separated by 60 km, both are on open sections of the coast and so should be subject to winds of similar magnitude. In addition, water stratification, a principal factor in the water column's response to winds, is similar at both sites during late winter and early spring. CTD measurements acquired over 1997–2000 indicate that during March–May, vertical stratification is very weak or absent off the Ontonagon and in the shelf area near the current meter. The current meter record can thus provide a rough sense of the wind-driven flow that may be expected in the Ontonagon discharge region during early spring and the extent to which this flow may advect the emerging river water.

Comparing the current meter record with the wind record from buoy 45006 (Fig. 11) indicates that springtime flows over the Keweenaw shelf are wind dominated. Fluctuations in alongshore currents measured in April and May show high visual correlation with fluctuations in the alongshore component of wind velocity. To quantify the wind-driven current at this site, we have used a standard technique (Bendat and Piersol 1971) to extract the wind-driven contribution of the alongshore current. The procedure involved first computing a two-input spectral transfer function relating the alongshore

and across-shore components of the surface wind stress (inputs) with the alongshore current velocity. The transfer function was then combined with the wind stress components to obtain the alongshore current response to the wind. This estimated response reaches magnitudes of close to 20 cm s^{-1} in both directions (Fig. 11), which accounts for 65% of the overall current variance. Wind-driven coastal currents of this magnitude are commonly seen in the Great Lakes (Csanady and Scott 1974; Murthy and Dunbar 1981).

If the Ontonagon plume is principally carried by the wind-driven flow, then the frequent reversals of this current should effectively limit the length of the plume by restricting the time it is advected in any particular direction. To illustrate this effect, and to gain a sense of how far the wind-driven coastal current may carry the Ontonagon discharge, we consider a displacement time series computed from the wind-driven current time series. The displacement series is defined as

$$Y(t) = \int_{t-T_D}^t v_w(t') dt'$$

where v_w is the alongshore wind-driven current and $Y(t)$ is the alongshore displacement of a fluid parcel carried by this current over the period $t - T_D$ to t . Comparing the displacement time series computed with $T_D = 2, 4,$ and 8 d (Fig. 11, bottom panel) clearly reveals the effect of current reversals on alongshore displacement. It is particularly notable that a fourfold increase in T_D , from 2 to 8 d, increases the root mean square (rms) displacement by only 55%, from 11 to 17 km.

To relate these displacements to possible plume advection distances, it is useful to estimate the time, T_S , over which the turbidity of a discharge plume element may be expected to be distinguishable from turbidity of surrounding water. For simplicity, we have estimated T_S by assuming that the particle concentration in a plume element is reduced by particle settling only. It was further assumed that particles in the plume settled at the Stokes velocity and were initially uniformly distributed over 20 m. T_S was taken as the time over which the suspended mass in a plume element was reduced, by settling, to 10% of its initial value. With these criteria and the particle size distributions from the discharge plume samples, T_S values with a mean of roughly 4 d were computed.

The direction shifts of the wind-driven alongshore flow may often produce two opposing plumes appearing to originate from the Ontonagon, an “active” plume of water being carried from the river mouth in the wind-driven current and a remnant plume carried in the opposite direction before the most recent current shift. Our survey measurements reveal this sort of arrangement, with an active plume stretching to the southwest of the river mouth and what may be a less turbid remnant plume extending to the northeast. The latter could be the result of alongshore flow generated by the winds of 25–28 March. The Devils Island winds have an eastward component in excess of 8 m s^{-1} over half this period.

Satellite-derived images of surface reflectance also frequently show bands of turbid water extending alongshore in

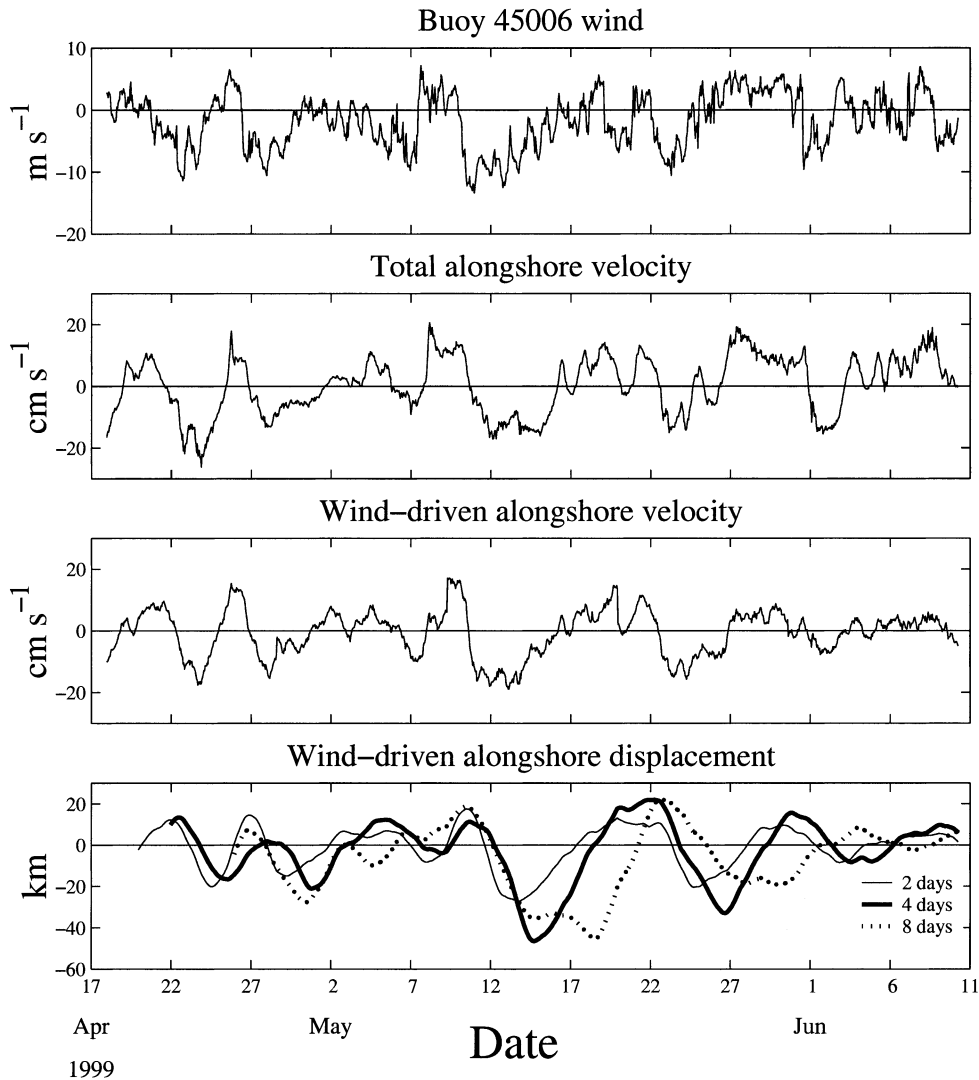


Fig. 11. The top three panels show the alongshore component of wind measured at buoy 45006 (Fig. 1), the alongshore component of velocity measured at the site off the central portion of Keweenaw peninsula (Fig. 1), and the estimated wind-driven portion of this current. Shown in the bottom panel are estimates of the alongshore distance the wind-driven current would carry fluid parcels over the indicated time intervals.

both directions from the Ontonagon River mouth. The image of 30 March 2000, the date of the fine-scale survey, offers a clear example of this (Fig. 12). This image is consistent with our survey results in that it shows the less turbid plume to the northeast.

Discussion

An important finding of our study is the significant impact of suspended particles on the density structure of the Ontonagon discharge plume. At the plume edge, our measurements show gradients in temperature and suspended particles making comparable contributions to the across-front gradients in density and to the associated geostrophic velocity. This may be typical of river discharges into large lakes during spring. Because of the small temperature differences be-

tween river and lake water that may be expected during this season, suspended particles carried in the river flow may be an important, and sometimes dominant, contributor to the river plume's buoyancy. The vertical movement of particles could thus play an important role in the dynamics of a river plume. During times of maximum discharge, for example, the rapid settling of larger particles near the river mouth may significantly alter density gradients and thus change the local momentum balance. It follows that numerical models of river discharge into large lakes during spring must carefully account for the behavior of suspended particles.

Our analysis reveals another property of the Ontonagon discharge that may be common to the flow of many rivers entering large lakes. Because of the small scale of the Ontonagon river mouth, the emerging river water is effectively impervious to the effects of the Earth's rotation. Its move-

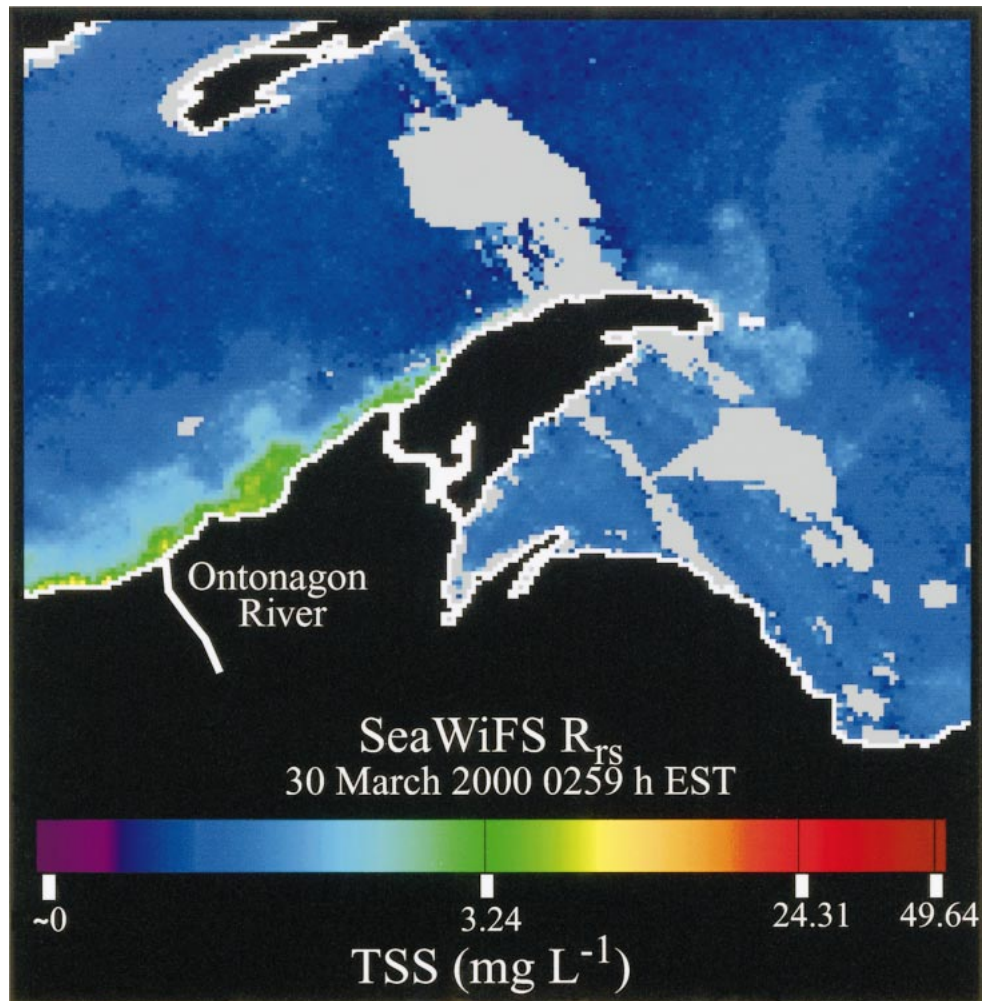


Fig. 12. SeaWiFS (sea-viewing wide field-of-view sensor) image of the Ontonagon River region of Lake Superior on 30 March 2000 showing turbid water bands extending alongshore in both directions from the Ontonagon River Mouth. The total suspended solids (TSS) was derived from remote sensing reflectance using the empirical relationship developed by Warrington (2001).

ment appears to be principally controlled by the local coastal current, which is of a scale large enough to be influenced by the Earth's rotation (as illustrated by the momentum balance calculation). During early spring, this current is principally driven by the surface wind stress. Our analysis suggests that the frequent reversals in the wind-driven flow may effectively limit the alongshore extent of the plume. The resulting reversals in the alongshore direction of the plume's motion may also create a near-shore turbid water band extending in both directions from the river mouth. In our study, the emerging plume is apparently embedded in such a turbid water band.

Our observations of a weak and nearly geostrophic velocity less than 1.5 km from the river mouth suggest that the emerging river water may rapidly adjust to a near-geostrophic dynamic balance. It also suggests that the momentum carried by the river water during our study period has little impact on the near-shore momentum balance. This may not always be the case, however. Our measurements cover a pe-

riod of modest river discharge. River transport during peak discharge can be a factor of five greater than that occurring during our study period. By dividing the river transport measured at the USGS Rockland, Michigan, station (Fig. 1) by the river mouth cross-section, we estimate that the Ontonagon River flow of the 1999 peak discharge would have a mean velocity of at least 1 m s^{-1} at the river mouth. The associated momentum flux of such a current could significantly impact the momentum balance at a considerable distance from the river mouth. In a study of the Niagara River plume, Masse and Murthy (1990) found that the near-source plume momentum balance was often dominated by the momentum flux of the emerging river flow. An examination of the outflow from the Leschenault estuary into Koombana Bay, Australia, by Luketina and Imberger (1987) revealed that the initial momentum flux of the estuarine flow formed a turbulent jet that could extend up to 2 km into the bay. In addition to momentum, the peak Ontonagon discharge will likely carry a significant suspended particle load. As noted

above, the settling of this could significantly impact plume dynamics. Clearly, the near-source dynamics of peak Ontonagon discharge may be significantly different, and far more complicated, than the near-source dynamics observed in our study. An understanding of plume dynamics during peak river discharge must thus await further investigation.

References

- BENDAT, J. S., AND A. G. PIERSOL. 1971. Random data: Analysis and measurement procedures. Wiley.
- BOICOURT, W. C., AND OTHERS. 1987. Physics and microbial ecology of a buoyant estuarine plume on the continental shelf. *EOS* **68**: 666–668.
- BOWMAN, M. J., AND R. L. IVERSON. 1977. Estuarine and plume fronts, p. 87–104. *In* M. J. Bowman and W. E. Esaias [eds.], *Oceanic fronts and coastal processes*. Springer.
- CHAO, S. 1998. Hyperpycnal and buoyant plume from a sediment-laden river. *J. Geophys. Res.* **103**: 3067–3081.
- CHEN, C. T., AND F. J. MILLERO. 1986. Precise thermodynamic properties for natural waters covering only the limnological range. *Limnol. Oceanogr.* **31**: 657–662.
- , J. ZHU, E. A. RALPH, S. A. GREEN, J. W. BUDD, AND F. Y. ZHANG. 2001. Prognostic modeling studies of the Keweenaw current in Lake Superior. Part I: Formation and evolution. *J. Phys. Oceanogr.* **31**: 379–395.
- CHURCHILL, J. H., J. O. BLANTON, J. L. HENCH, R. A. LUETTICH, AND F. E. WERNER. 1999. Flood tide circulation near Beaufort Inlet, North Carolina: Implications for larval recruitment. *Estuaries* **22**: 1057–1070.
- CSANADY, G. T. 1982. Circulation in the coastal ocean. Reidel.
- , AND J. T. SCOTT. 1974. Baroclinic coastal jets in Lake Ontario during IFYGL. *J. Phys. Oceanogr.* **4**: 524–541.
- DAVIS, R. E. 1985. Drifter observations of coastal surface currents during CODE: The method and descriptive view. *J. Geophys. Res.* **90**: 4741–4755.
- GARVINE, R. W. 1987. Estuary plumes and fronts in shelf waters: A layer model. *J. Phys. Oceanogr.* **17**: 1877–1896.
- . 1995. A dynamical system for classifying buoyant coastal discharges. *Cont. Shelf Res.* **15**: 1585–1596.
- , AND J. D. MONK. 1974. Frontal structure of a river plume. *J. Geophys. Res.* **79**: 2251–2259.
- GATZKE, T. M. 2001. Interaction of the spring runoff event with the thermal bar in Lake Superior. M.S. thesis, Michigan Technological University.
- GAWARKIEWICZ, G., F. BAHR, R. C. BEARDSLEY, AND K. H. BRINK. 2001. Interaction of a slope eddy with the shelfbreak front in the Middle Atlantic Bight. *J. Phys. Oceanogr.* **31**: 2783–2796.
- HICKEY, B. M., L. J. PIETRAFESA, D. A. JAY, AND W. C. BOICOURT. 1998. The Columbia river plume study, subtidal variability in the velocity and salinity fields. *J. Geophys. Res.* **103**: 10339–10368.
- LUKETINA, A. A., AND J. IMBERGER. 1987. Characteristics of a surface buoyant jet. *J. Geophys. Res.* **92**: 5435–5447.
- MASSE, A. K., AND C. R. MURTHY. 1990. Observations of the Niagara River thermal plume (Lake Ontario, North America). *J. Geophys. Res.* **95**: 16,097–16,109.
- MUNCHOW, A., AND R. W. GARVINE. 1993. Dynamical properties of a buoyancy driven coastal current. *J. Geophys. Res.* **98**: 20,063–20,077.
- MURTHY, C. R., AND D. S. DUNBAR. 1981. Structure of the flow within the coastal boundary layer of the Great Lakes. *J. Phys. Oceanogr.* **11**: 1567–1577.
- NUNES VAZ, R. A., G. W. LENNON, AND D. G. BOWERS. 1990. Physical behavior of a large, negative or inverse estuary. *Cont. Shelf Res.* **10**: 277–304.
- O'DONNELL, J., G. O. MARMORINO, AND C. L. TRUMP. 1998. Convergence and downwelling at a river plume front. *J. Phys. Oceanogr.* **28**: 1481–1495.
- RAGOTZKIE, R. A. 1966. The Keweenaw Current, a regular feature of summer circulation in Lake Superior. Technical Report 29, University of Wisconsin Department of Meteorology.
- VIEKMAN, B. E., AND M. WINBUSH. 1993. Observations of the vertical structure of the Keweenaw Current, Lake Superior. *J. Great Lakes Res.* **19**: 470–479.
- WARRINGTON, D. S. 2001. Great Lakes chlorophyll and turbidity estimates using SeaWiFS (sea-viewing wide field-of-view sensor) imagery. M.S. thesis, Michigan Technological University.
- WILLIAMS, A. J., J. S. TOCHKO, R. L. KOEHLER, W. D. GRANT, T. F. GROSS, AND C. V. R. DUNN. 1987. Measurement of turbulence in the oceanic bottom boundary layer with an acoustic current meter array. *J. Atmos. Ocean. Tech.* **4**: 312–327.
- WRIGHT, L. D., Z.-S. YANG, B. D. BORNHOLD, G. H. KELLER, D. B. PRIOR, AND W. J. WISEMAN. 1986. Hyperpycnal plumes and plume fronts over the Huanghe (Yellow River) Delta Front. *Geol. Mar. Lett.* **6**: 97–105.
- WU, J. 1969. Windstress and surface roughness at the air-sea interface. *J. Geophys. Res.* **74**: 444–445.
- ZHU, J., C. CHEN, E. A. RALPH, S. A. GREEN, J. W. BUDD, AND F. Y. ZHANG. 2001. Prognostic modeling studies of the Keweenaw current in Lake Superior. Part II: Simulation. *J. Phys. Oceanogr.* **31**: 396–410.

Received: 21 August 2001

Accepted: 6 April 2002

Amended: 4 November 2002